

Research Article

Fuzzy PI Controller Based Fault Analysis and Recovery in Sensorless BLDC Motor using High Gain Hybrid Converter (HGHC)

¹R. Jayanthi and ²I. Gnanambal

¹SCSVMV University, Enathur, Kanchipuram-631561,

²Government College of Engineering, Salem-636011, Tamil Nadu, India

Abstract: Renewable Energy Sources (RES) has been widely used in various applications due to increase in power demand. In this study, a High Gain Hybrid Converter (HGHC) has been used to utilize maximum power from PV panel and to control the battery mode of operation such as charging/discharging in an efficient manner. In the load side, sensor less BLDC motor has been used in this study. After the back EMF is generated in the load side BLDC motor, it is taken as feedback to the HGHC. So, this will act as the main supply and thus, more power can be saved. Moreover, this research study also focuses on the transient analysis of the BLDC motor. The inverter in BLDC motor plays a vital role as it is responsible for flux generation and fixing up of angle 'θ' to the motor for its operation. So, the failures in the switches of the inverter would greatly affect the overall functioning of the BLDC motor. Thus, this research study focuses on the failure analysis of these switches in the inverter. In order to analyze and recover these faults, error controllers have been used in this proposed study. The simulations are carried out in MATLAB r2011a and the results are taken. The results show the significant performance of the proposed model.

Keywords: BLDC motor, High Gain Hybrid Converter (HGHC), PI and fuzzy controllers

INTRODUCTION

For the past two decades several Asian countries such as Japan, which have been under pressure from high energy prices, have implemented variable speed PM motor drives for energy saving applications such as air conditioners and refrigerators (Kinjo *et al.*, 2006). On the other hand, the U.S.A., has kept on using cheap induction motor drives, which have around 10% lower efficiency than adjustable PM motor drives for energy saving applications. Therefore recently, the increase in energy prices spurs higher demands of variable speed PM motor drives. Also, recent rapid proliferation of motor drives into the automobile industry, based on hybrid drives, generates a serious demand for high efficient PM motor drives and this was the beginning of interest in BLDC motors.

The present decade has seen increased usage of renewable energy in various home and industrial applications due to its power conservation and increased power demand. The main issues faced by the developers in these applications are the handling of a high output dc-voltage across the dc bus and also achieving high current before supplying to the inverter (Kinjo *et al.*, 2006).

The battery is charged from the PV panel and in order to utilize the supply from the battery and the PV panel, a higher number of conversion stages are required. Because of these higher number of conversion

stages, more number of semiconductor devices would be required which in turn would result in huge size, high cost, higher power losses, voltage and current stress across the semiconductor devices such as switch, diode, capacitor, inductor, etc., (Bouzelata *et al.*, 2012).

Thus, in this research study, for utilizing maximum power from the PV panel, battery charging and efficient recovery of battery power, a proficient dc-dc converter with single conversion stage is proposed for better overall performance. The present research study focuses on efficient battery charging based on the proposed hybrid converter. This utilized power can be supplied to AC or DC motor drives with efficient energy consumption (Luiz *et al.*, 2014).

In recent years, most of the Asian countries are suffering from high energy prices which have implemented variable speed PM motor drives for energy saving applications such as air conditioners, fuel pump and refrigerators (Iizuka *et al.*, 1985; Gamazo-Real *et al.*, 2010). But, countries like U.S.A., are continuously using induction motor drives, which consume higher power than the adjustable PM motor drives for energy saving applications. Therefore recently, the higher energy prices results in higher demands of variable speed PM motor drives. Moreover, sudden and fast explosion of motor drives into various industries formulates a higher demand for high efficient PM motor drives and thus BLDC motors have been an attractive research area.

BLDC motors have several unique features and benefits when compared with brushed DC motors and induction motors. The main advantageous aspects are the better speed versus torque characteristics, high dynamic response, high efficiency and reliability, long operating life, noiseless operation, higher speed ranges and reduction of Electromagnetic Interference (EMI). The control of BLDC motors can be carried out in sensor or sensor less mode, but in order to minimize the overall cost of devices, sensor less control approaches have been preferred as it eliminates the sensing part. The disadvantages of sensor less control are higher requirements for control algorithms and more complicated electronics (Hubik *et al.*, 2008).

In real time scenarios, AC Induction Motor can be used in analyzing the behavior of the Insulation Conductivity Resistance (IRC) of the hot air chamber is most of the industries. But, the main limitation of the AC Induction Motor is that, it has power consumption, high torque, higher noise and huge size (Zhenyu, 2012). In this application, BLDC motor can be used to analyze the variation behavior of IRC and based on this examination, the hot air inside the chamber can be sprayed at varying temperatures. This would in turn facilitate lesser power consumption, lesser noise and size.

This research study focuses on deciding the mode of operation of converters i.e., Buck (charging), Boost (discharging), analysis of speed-torque relational and Back EMF feedback method for converter with different type of error controllers such as PI, Fuzzy and hybrid Fuzzy-PI. Moreover, in the load side, this study concentrates on the speed control of the BLDC motor, fault analysis with single and dual leg switch failure and fault recovery with the support of alternate switches.

LITERATURE REVIEW

The author introduces a new circuit topology and a dc link voltage control approach to maintain incoming and outgoing phase currents varying at the similar rate during commutation (Tingna *et al.*, 2010). A dc-dc Single-Ended Primary Inductor Converter (SEPIC) and a switch selection circuit are used before the inverter. The preferred commutation voltage is proficient through the SEPIC converter. The dc link voltage control approach is processed by the switch selection circuit to divide two procedures, tuning the SEPIC converter and regulating speed. The cause of commutation ripple is examined and the way to obtain the desired dc link voltage is commenced in detail. Lastly, simulation and experimental results show that, compared with the dc-dc converter, the proposed method achieves the desired voltage much earlier and reduces commutation torque ripple more resourcefully at both high and low speeds.

In Alaeinovin and Jatskevich (2012) Brushless dc motors controlled by Hall-effect sensors are employed

in variety of applications, in which the Hall sensors should be placed 120 electrical degrees at a distance. This is complex to attain in practice particularly in low-precision motors, which leads to unsymmetrical operation of the inverter/motor phases. To lessen this happening, an approach of filtering the Hall-sensor signals has been proposed recently. This note extends the earlier work and proposes a very well-organized digital implementation of such filters that can be simply incorporated into various brushless dc motor-drive systems for restoring their operation in steady state and transients.

An automatic system for fault diagnosis and position of stator-winding inter turns in permanent-magnet brushless dc motors is introduced. System performances beneath well and damaged operation are obtained by means of a discrete-time model. Waveform of the electromagnetic torque is monitored and functioned by means of discrete Fourier transform and short-time Fourier transform to develop appropriate diagnostic indices. Two Adaptive Neuro-Fuzzy Inference Systems (ANFIS) are designed to computerize the fault diagnosis procedure (Awadallah and Morcos, 2004).

This study introduces a well-organized and robust control method for the position-sensor less Electric Vehicle (EV) by means of a brushless dc motor. The back electromotive force detection technique is initially take on and enhanced to implement sensor less control of the motor. The equivalent circuits of the control system are represented and the mathematical models underneath normal driving and energy regeneration are then derived, correspondingly. By combining the benefits of nonsingular terminal sliding mode with the high-order sliding-mode technique, a Hybrid Terminal Sliding-Mode (HTSM) control scheme for EV is put forward to assurance both system performance and robust stability (Yaonan *et al.*, 2011).

PROPOSED BLDC MOTOR ARCHITECTURE

The overall proposed architectural framework of the sensor less BLDC motor is shown in Fig. 1. The Voltage Source Inverter (VSI) in BLDC motor plays an essential role as it is responsible for flux generation and fixing up of angle ' θ ' to the motor for its operation. Based on the principle of BLDC motor, there would be supply along two phases. Along one phase, back emf would be generated. These back emf are sensed which generates the pulse after zero crossing detection which is the position encoding. Based on the switching table, the decision regarding the operation of switches can be controlled.

In this proposed architecture, the converter also has an essential role as it affects the overall performance of the system. A High Gain Hybrid Converter (HGHC) is used in this approach. The essential aspects involved in this HGHC include PV panel, battery, effective back

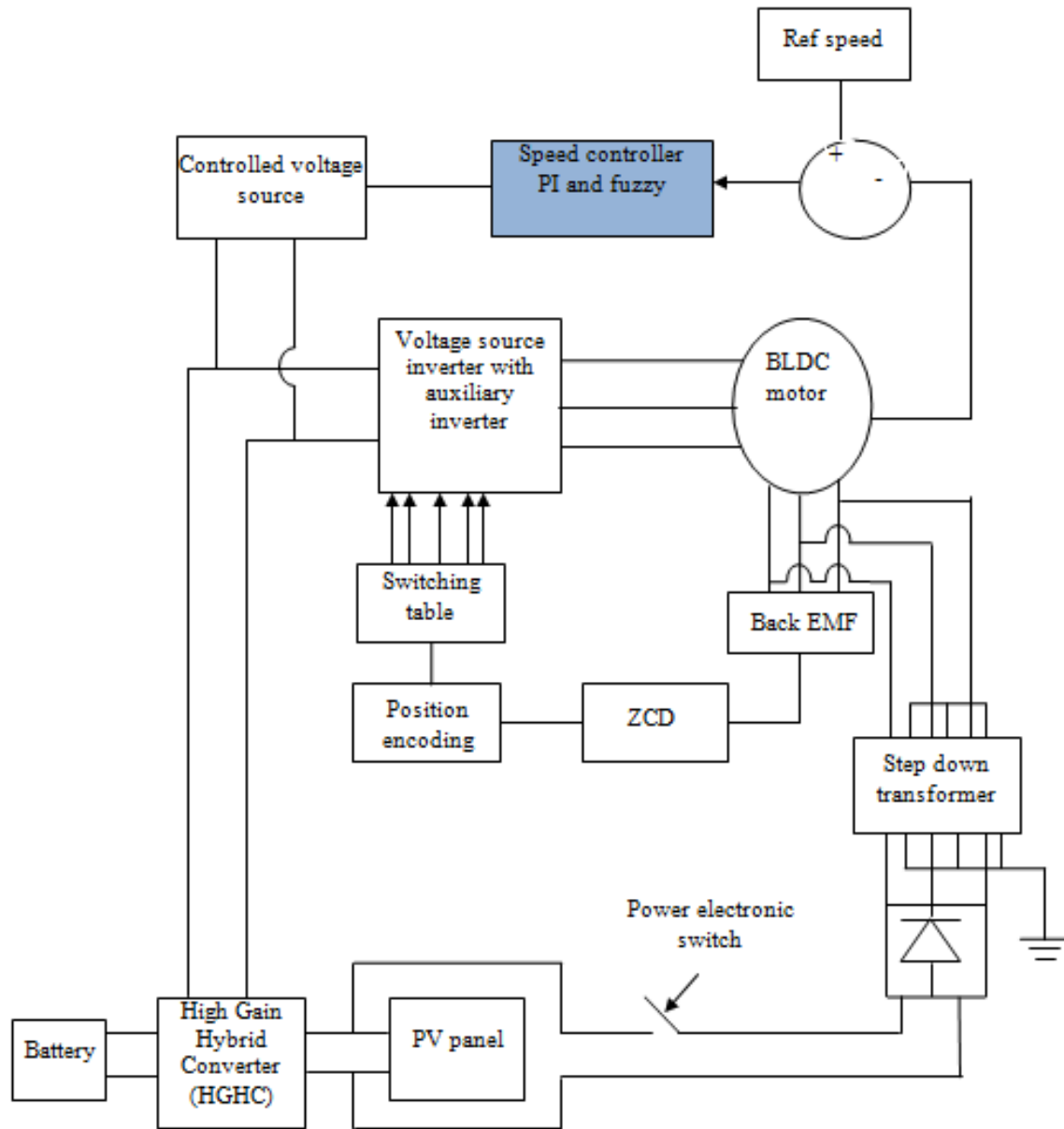


Fig. 1: Proposed architecture methodology

emf feedback method and load handling mechanisms. Initially, PV panel has been used in order to generate a general supply current. Once, the current get generated, based on the modes of operation of HGHC, the battery gets charged and it also supports the load, if there is excess power.

Once the current is fed to the BLDC motor, a back emf is generated simultaneously which varies with different position values. Thus, after the back emf is generated, a primary winding of the step down transformer is used to collect the back emf as shown in the Fig. 1.

This collected back emf/voltage is converted into a DC supply through uncontrolled diode rectifier. This

DC voltage is given as input to the HGHC which in turn charges the battery and supports the load. Once, the PV panel does not generate required power of the load, the back emf DC voltage itself supports the load. Thus, this architecture is very useful as it has efficient energy management with battery charging capability and it acts as a UPS system.

BLDC motor modeling: Modeling of a BLDC motor can be developed in the similar manner as a three-phase synchronous machine. Since there is a permanent magnet mounted on the rotor, some dynamic characteristics are different. Flux linkage from the rotor depends upon the magnet material. Therefore,

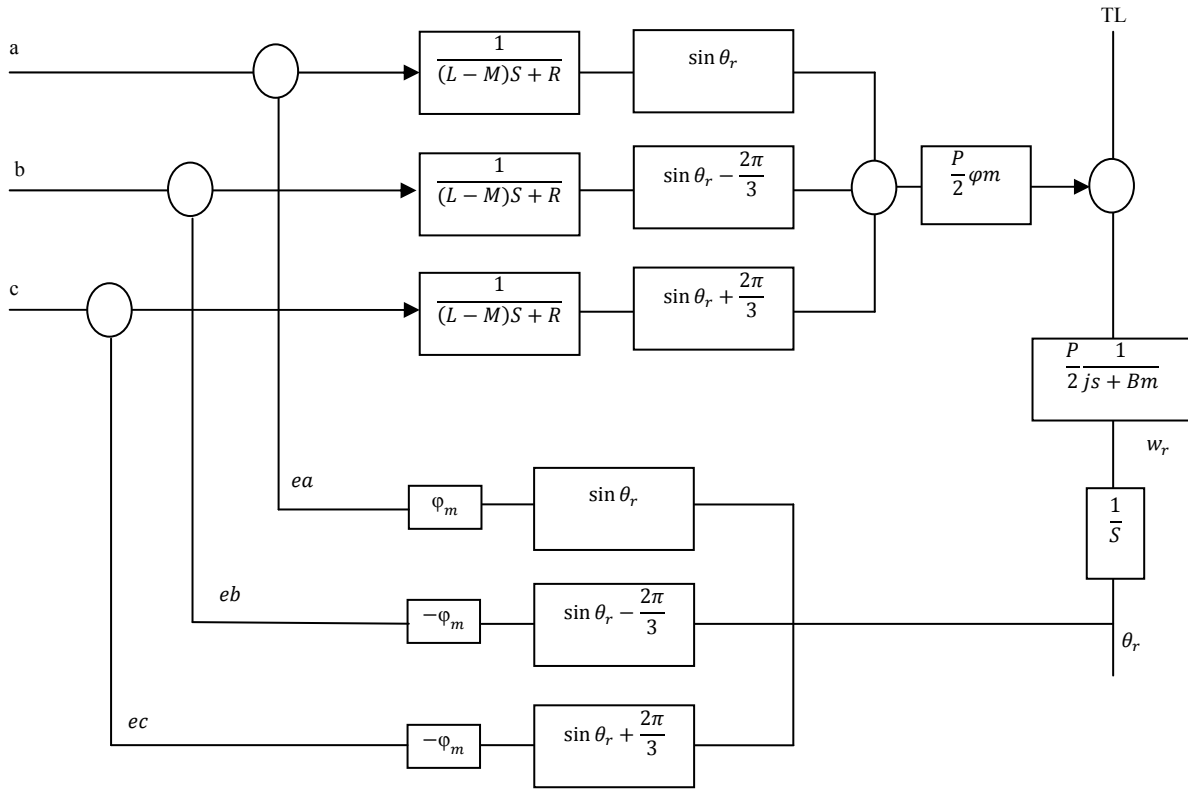


Fig. 2: BLDC modeling

saturation of magnetic flux is typical for this kind of motors. As any typical three-phase motors, one structure of the BLDC motor is fed by a three phase voltage source (Je-Wook *et al.*, 2013):

$$V_a = iaRa + \frac{d}{dt} [La ia + Lab ib + Lac ic] + ea$$

$$V_b = iaRb + \frac{d}{dt} [Lba ia + Lb ib + Lbc ic] + eb$$

$$V_c = icRc + \frac{d}{dt} [Lca ia + Lcb ib + Lc ic] + ec$$

where,

- L = Armature self-inductance (H)
- R = Armature resistance (Ω)
- V_a, V_b, V_c = Terminal phase voltage (V)
- ia, ib, ic = Motor input current (A)
- P = Number of poles
- θ_r = The rotor position of the motor

Figure 2 clearly shows the modeling of the BLDC motor which shows that integration of the speed provides rotor position θ , which is then phase shifted through $0, -\frac{2\pi}{3}$ and $\frac{2\pi}{3}$ and multiplied with sine to attain the back emf ea, eb and ec .

Back EMF: Let In the 3-phase BLDC motor, the back-EMF is related to a function of rotor position and the rotor position and the back-EMF of each phase has 120o phase angle difference so equation of each phase should be as follows:

$$ea = -wr \phi_m \sin Dr$$

$$eb = -wr \phi_m \sin (Dr - \frac{2\pi}{3})$$

$$ec = -wr \phi_m \sin (Dr - \frac{4\pi}{3})$$

Where, ea, eb, ec represents the motor back-EMF (V):

$$\frac{d}{dt} ia = \frac{1}{(L - m)} (V_a - iaRa) + \phi_m wr \sin Dr$$

$$\frac{d}{dt} ib = \frac{1}{(L - m)} (V_b - ibRb) + \phi_m wr \sin (Dr - \frac{2\pi}{3})$$

$$\frac{d}{dt} ic = \frac{1}{(L - m)} (V_c - icRc) + \phi_m wr \sin (Dr - \frac{4\pi}{3})$$

The source is not necessarily to be sinusoidal. Square wave or other wave-shape can be applied as

long as the peak voltage does not exceed the maximum voltage limit of the motor. Similarly, the model of the armature winding for the BLDC motor is expressed as follows.

Electromagnetic torque: Total torque output can be represented as summation of that of each phase. Next equation represents the total torque output:

$$T_e = \frac{P}{\omega_m}$$

where, T_e is total torque output (Nm)

The equation of mechanical part is represented as follows:

$$P = e_a i_a + e_b i_b + e_c i_c$$

$$T_e = j \left(\frac{2}{p} \right) \frac{d}{dt} (\omega_r) + B_m \left(\frac{2}{p} \right) \omega_r + T_L$$

$$\omega_r = \frac{d}{dt} \theta_r$$

where,

T_L = Load torque (Nm)

B_m = The Damp coefficient

ω_r = Rotor Speed

j = Inertia

SPEED CONTROL TECHNIQUES

To achieve desired level of performance the motor requires suitable speed controllers. In case of permanent magnet motors, usually speed control is achieved by using Proportional-Integral (PI) controller. Although conventional PI controllers are widely used in the industry due to their simple control structure and ease of implementation, these controllers pose difficulties where there are some control complexity such as nonlinearity, load disturbances and parametric variations. Moreover PI controllers require precise linear mathematical models.

The speed of the motor is compared with its reference value and the speed error is processed in Proportional-Integral (PI) speed controller.

The main aim of tuning proportional gain (K_p) and K_i values are that in order to increase the rise time, K_p becomes essential. Similarly, in order to decrease settling time, peak overshoot, peak undershoots and steady state error, K_i is essential:

$$e(t) = \omega_{ref} - \omega_m(t)$$

$\omega_m(t)$ is compared with the reference speed ω_{ref} the resulting error is estimated at the nth sampling instant as:

$$T_{ref}(t) = T_{ref}(t-1) + K_p[e(t) - e(t-1)] + K_i e(t)$$

Where K_p and K_i are the proportional and Integral gains of PI speeds controller respectively. The output of this controller is considered as the reference torque. A limit is put on the speed controller output depending on permissible maximum winding currents. The reference current generator block generates the three phase reference currents i_a , i_b and i_c using the limited peak current magnitude decided by the controller and the position sensors.

Fuzzy logic controller: Fuzzy logic expressed operational laws in linguistics terms instead of mathematical equations. Many systems are too complex to model accurately, even with complex mathematical equations; therefore traditional methods become infeasible in these systems.

However fuzzy logics linguistic terms provide a feasible method for defining the operational characteristics of such system. Fuzzy logic controller can be considered as a special class of symbolic controller. The input variable is speed Error (E) and Change in speed Error (CE) is calculated by the controller with E. The output variable is the torque component of the reference (ref i) where ref i is obtained at the output of the controller by using the change in the reference current.

The fuzzy member's ship function for the input variable and output variable are chosen as follows:

- Positive Big: PB
- Negative Big: NB
- Positive Medium: PM
- Negative Medium: NM
- Positive Small: PS
- Negative Small: NS
- And zero: ZO

The input variable speed error and change in speed error is defined in the range of:

$$-1 \leq \omega_e \leq +1$$

$$-1 \leq \omega_{ce} \leq +1$$

and the output variable torque reference current change Δi_{qs} is define in the range of:

$$-1 \leq \Delta i_{qs} \leq +1$$

The triangular shaped functions are chosen as the membership functions due to the resulting best control performance and simplicity. The membership function for the speed error and the change in speed error and the change in torque reference current are shown

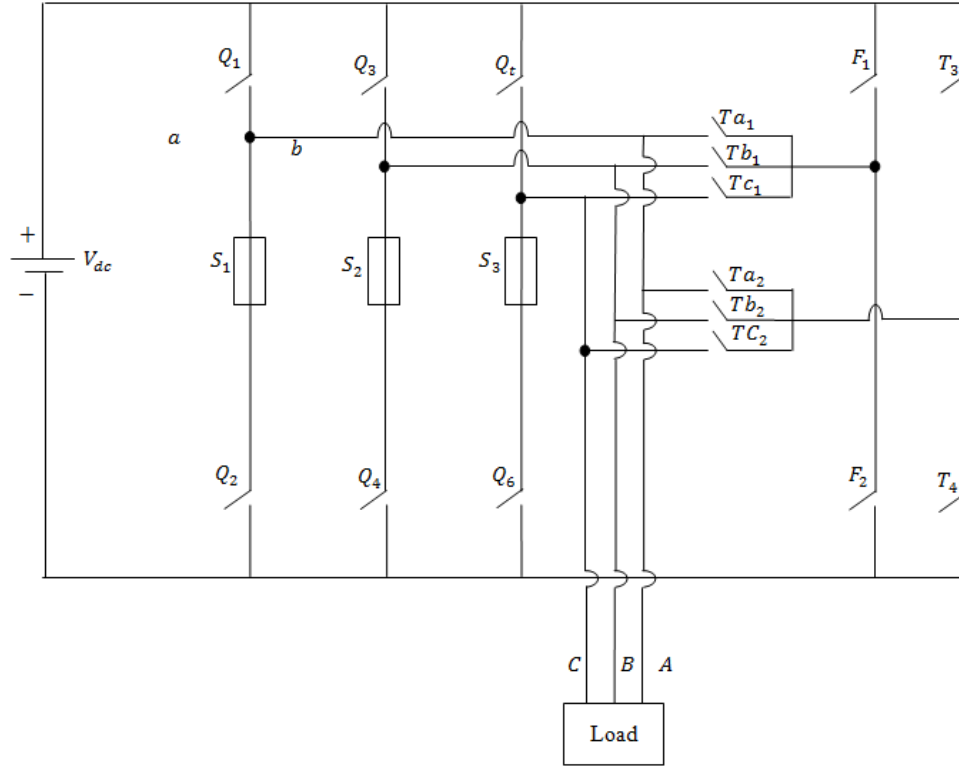


Fig. 3: Fault recovery modeling

Table 1: 7×7 fuzzy rule base

e/ce	NB	NM	NS	ZO	PS	PS	PB
NB	NB	NB	NB	NB	NM	NS	ZO
NM	NB	NB	NB	NM	NS	ZO	PS
NS	NB	NB	NM	NS	ZO	PS	PM
ZO	NB	NM	NS	ZO	PS	PM	PB
PS	NB	NS	ZO	PS	PM	PB	PB
PM	NM	ZO	PS	PM	PB	PB	PB
PB	NS	PS	PM	PB	PB	PB	PB

Table 2: Fault recovery switching table

I _a	I _b	I _c	T _{a1}	T _{b1}	T _{c1}	T _{a2}	T _{b2}	T _{c2}	F ₁	F ₂	F ₃	F ₄
0	-	-	1	0	0	0	0	0	Q ₁	Q ₂	0	0
-	0	-	0	1	0	0	0	0	Q ₃	Q ₄	0	0
-	-	0	0	0	1	0	0	0	Q ₅	Q ₆	0	0
0	0	-	1	0	0	0	1	0	Q ₁	Q ₂	Q ₃	Q ₄
-	0	0	0	1	0	0	0	1	Q ₃	Q ₄	Q ₅	Q ₆
0	-	0	1	0	0	0	0	1	Q ₁	Q ₂	Q ₅	Q ₆

(Fig. 3) for all variables seven levels of fuzzy membership function are used (Table 1).

FAULT ANALYSIS AND RECOVERY MODEL

In this approach, fault represents the switch failure in legs. So, when this failure occurs, the leg current becomes zero. When this condition occurs, the same operation has to be done through the auxiliary inverter based on the fault recovery switching table as soon in Table 2. Two sets of relay bypass switches have been used in this approach in order to avoid any technical issues if all the two switches in a same leg failed. The first sets relay bypass switch supports the first switch

and the second set relay switch supports the second switch in the same leg. This process protects the switches from short circuit in the same leg switching failure.

The statistical parameters of the segmented images in the Fig. 4 are represented in the Table 2 and 3. The main reason for adopting the conditional random field is computation probability and statistical parameter estimation is easy when compared to the existing Markov random field process. The segmented image of proposed method is evaluated using the metrics such as correlation, non-uniformity, similarity measure. The performance evaluation of the proposed method is better than the existing methods. The

Table 3: Mode 1 to mode 3

Circuit components	Mode 1	Mode 2	Mode 3
S1	OFF	-	-
S2	ON	-	ON
S3	OFF	-	ON (ZVS mode)
S4	ON	OFF (end of the time)	OFF (beginning time)
I_N	Increases linearly	Increases linearly	Decreases linearly
T2a	Decreases linearly	Null	Decreases linearly
T2c	Increases linearly	Null	Increases linearly
T1a	-	-	Increases linearly
T1b	-	-	Decreases linearly

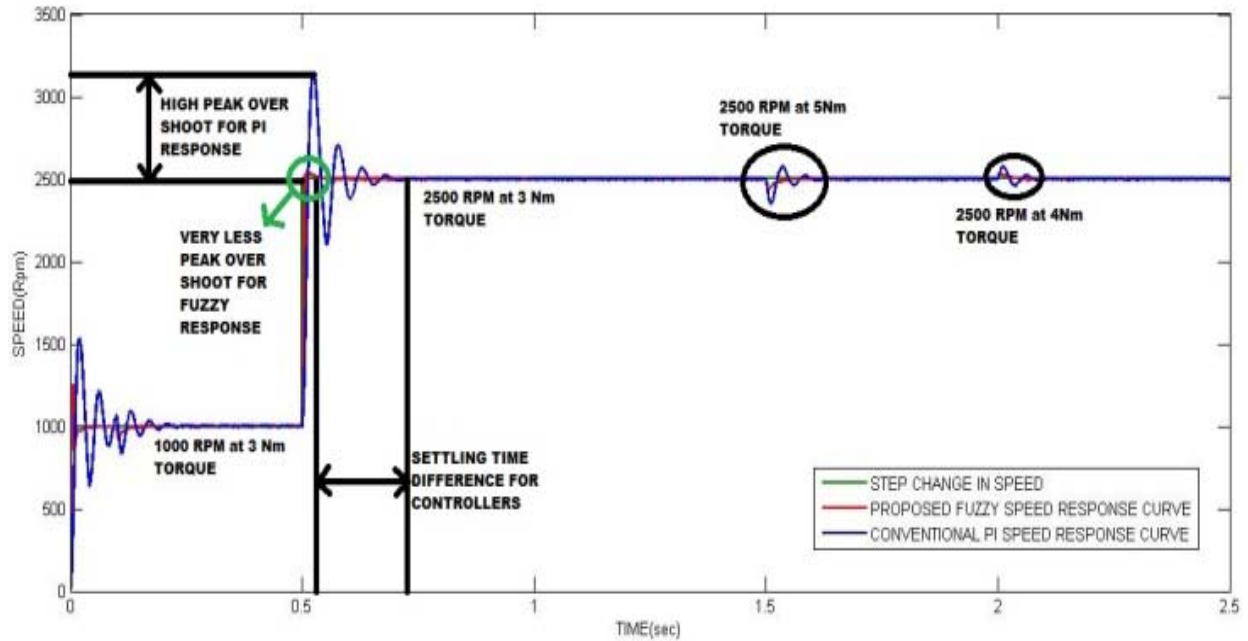
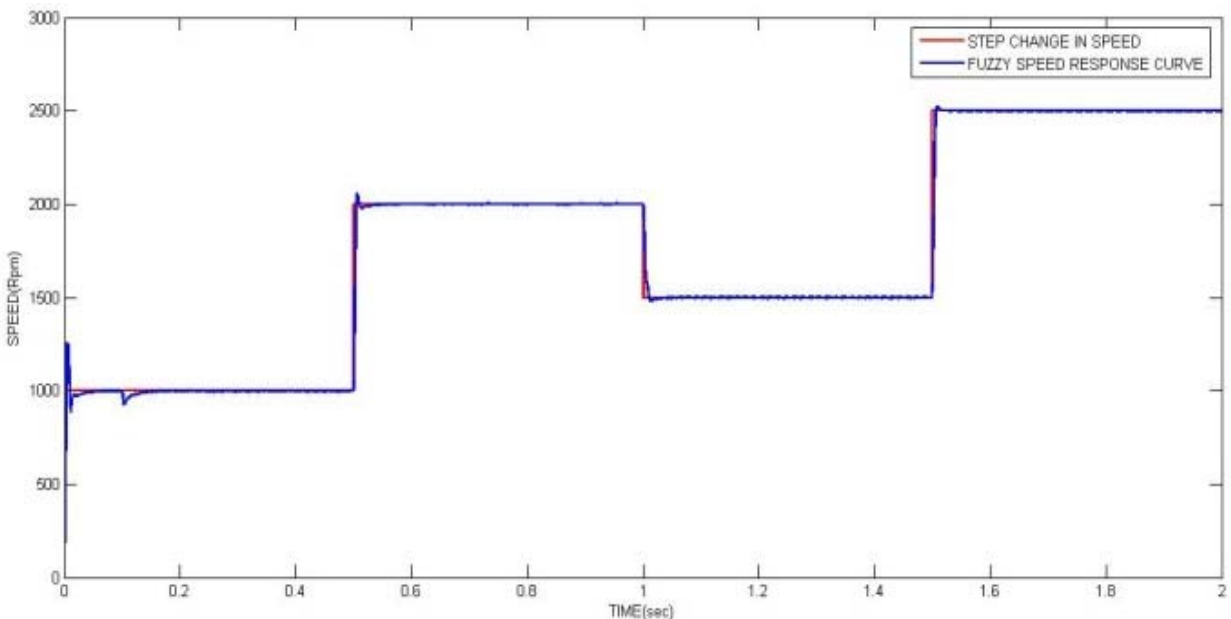
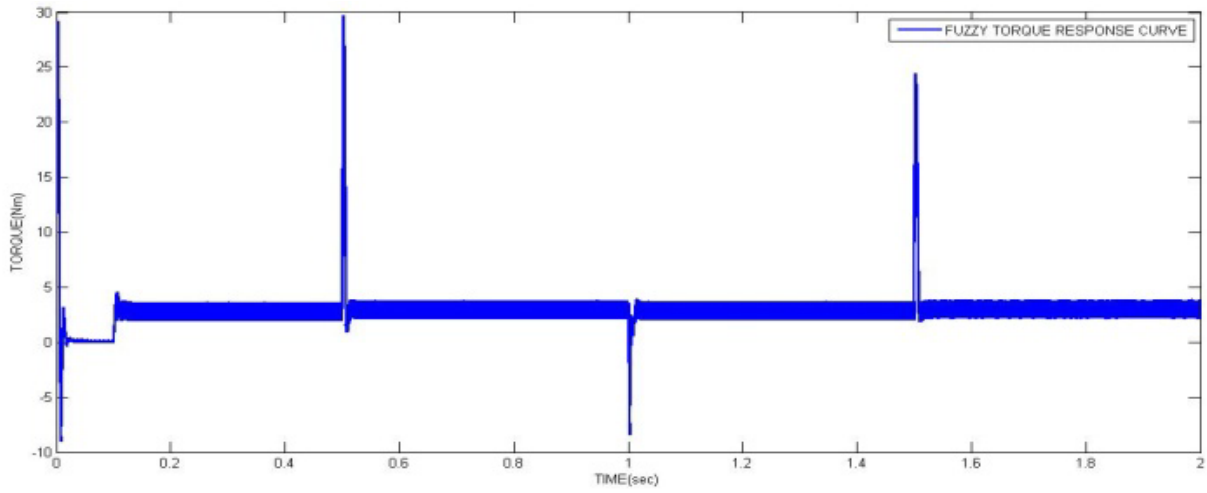


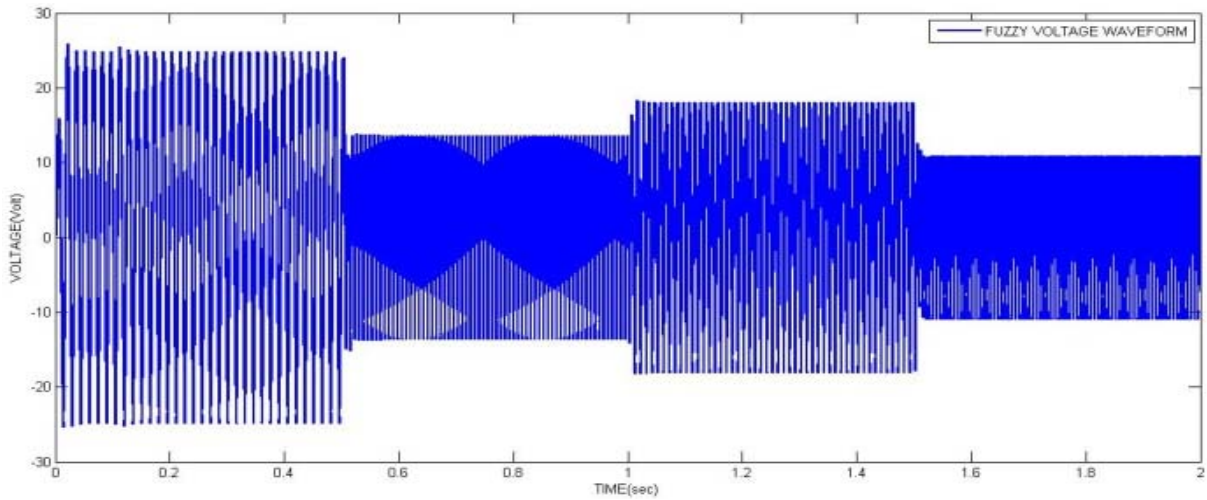
Fig. 4: Performance evaluation of two speed combined response



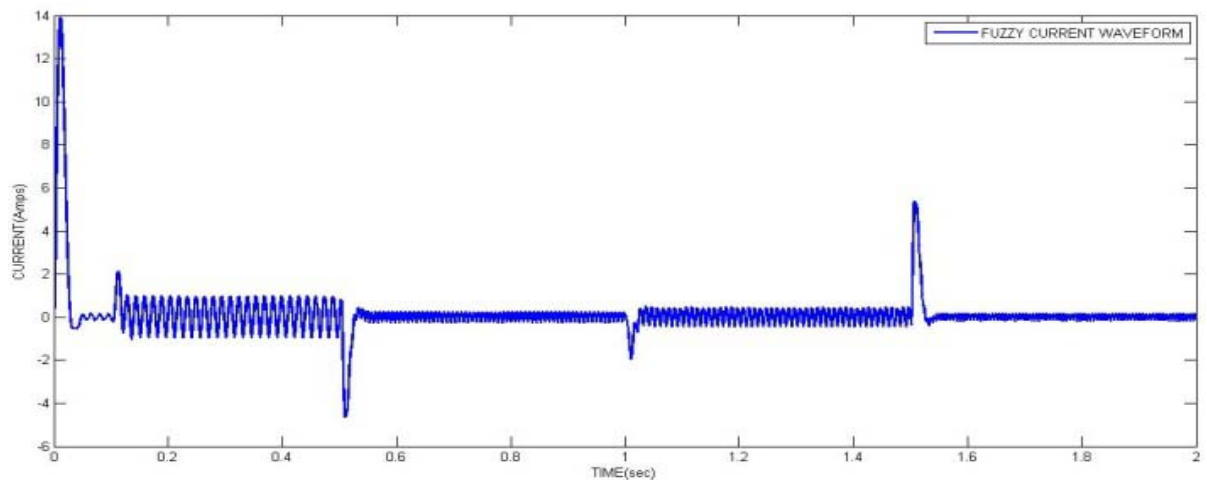
(a) Speed response



(b) Torque response



(c) Voltage response



(d) Current response

Fig. 5: Speed, torque, voltage and current response of fuzzy controller

graphical representation of the performance evaluation is shown in the (Fig. 5 to 8). The comparison results of existing and proposed methods are shown in the Table 1.

PROPOSED HIGH GAIN HYBRID CONVERTER

Converters and its mode of operation: The architectural diagram of the proposed HGHC is shown in Fig. 9. The proposed HGHC has two operation segments. The duty cycle is applied to the lower switches of each leg (S2 and S4), which operate in opposite phase. The converter behavior and the operation segment are based on the applied duty cycle. If the duty cycle is higher than 50%, the lower switches work in overlapping mode. But, if the duty cycle is

lower than 50%, then only the upper switches are in an overlapping mode. As the operation principle regarding the switches is analogous, only the case for $D > 50\%$ is presented (Alcazar *et al.*, 2013).

The converter presents six operation stages as represented in Table 3 and 4. As it can be observed, the current through the input inductor has a frequency which is twice higher than the switching frequency, which characterizes the three-state commutation cell behavior. This current is then equally shared between the windings of the autotransformers, which leads to reduced current stresses. The windings T2a and T2c correspond to the transformer primary side, which are responsible for stepping the voltage up and allowing the switches to operate in the ZVS mode, increasing the system efficiency (Torrico-Bascope *et al.*, 2006).

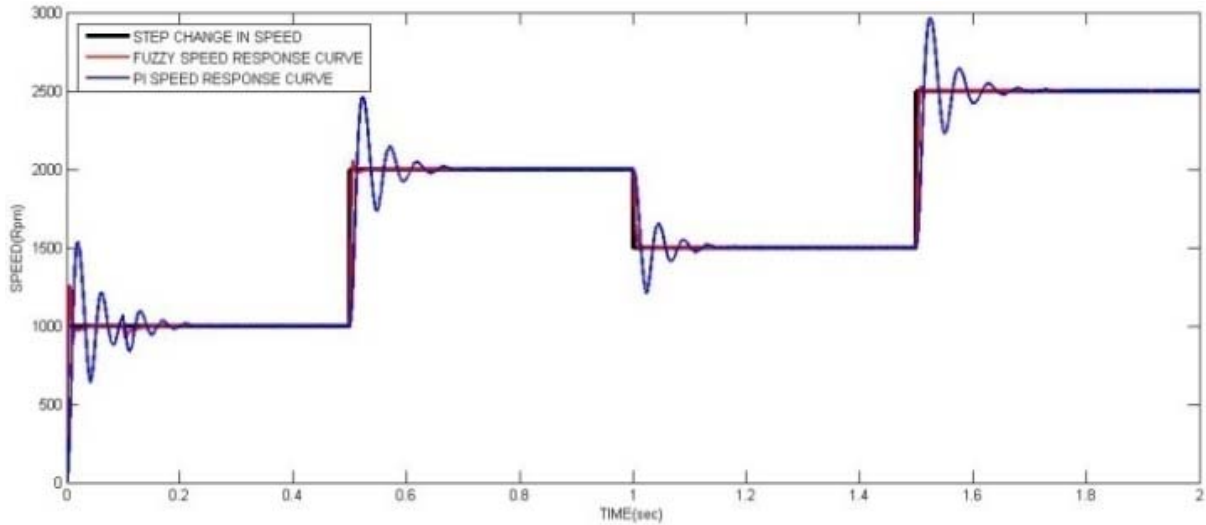


Fig. 6: Speed response comparison of PI and fuzzy controllers

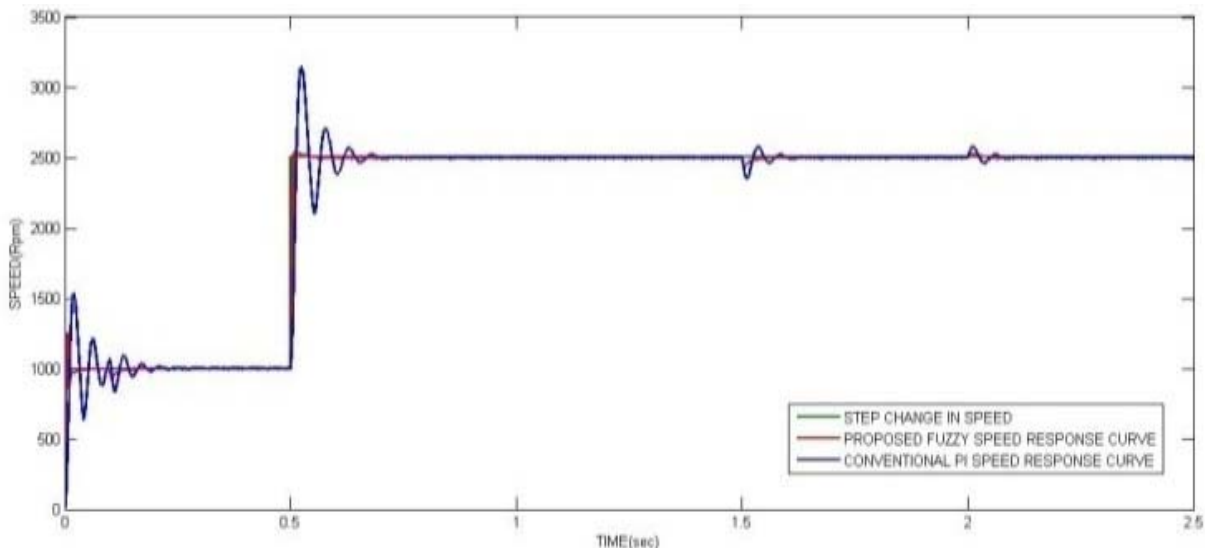


Fig. 7: Sudden change in speed with sudden change in torque

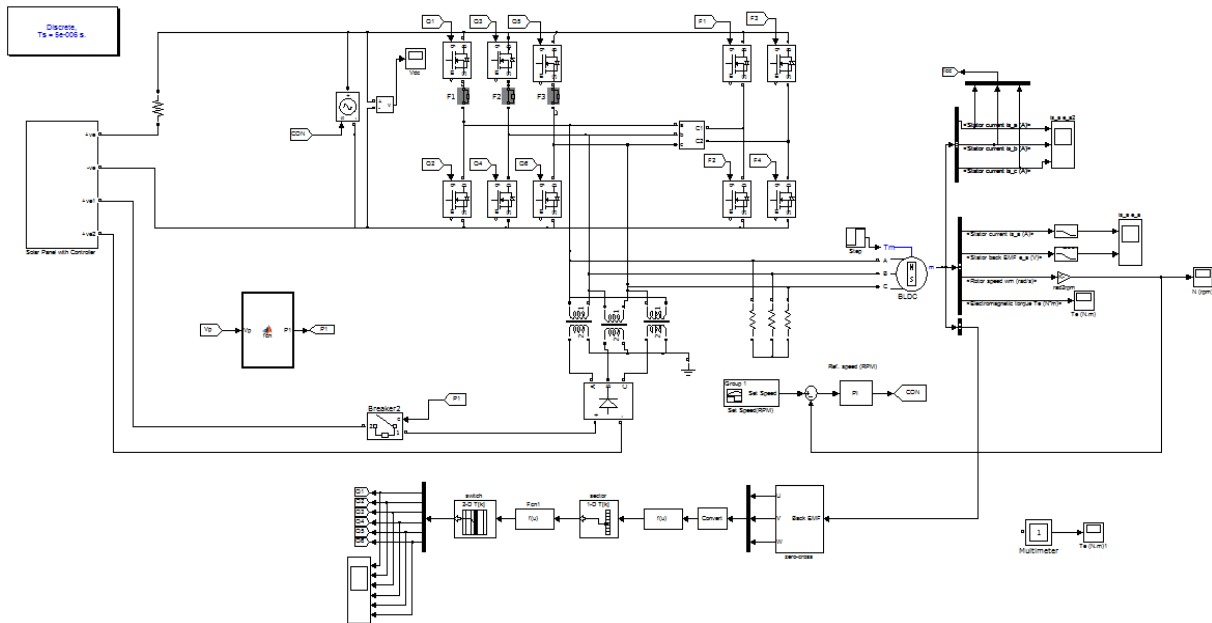


Fig. 8: Proposed simulation diagram

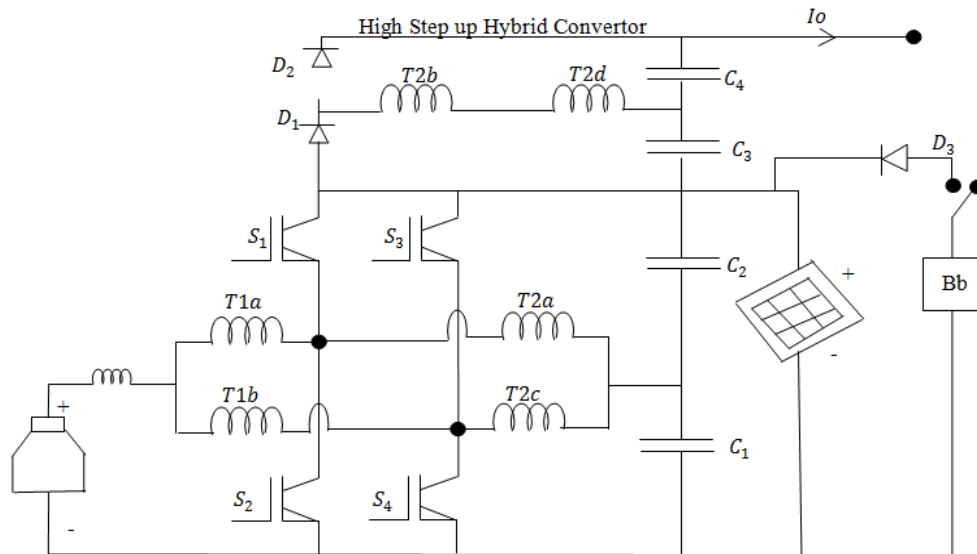


Fig. 9: Proposed high gain hybrid converter

Table 4: Mode 4-mode 6

Circuit components	Mode 4	Mode 5	Mode 6
S1	-	-	ON (ZVS mode)
S2	ON	OFF (end of the time)	OFF (beginning time)
S3	-	-	OFF
S4	ON	-	ON
I IN	Increases linearly	Increases linearly	Decreases linearly
T2a	Increases linearly	Null	Increases linearly
T2c	Decreases linearly	Null	Decreases linearly
T1a	Increases linearly	-	-
T1b	Increases linearly	-	-

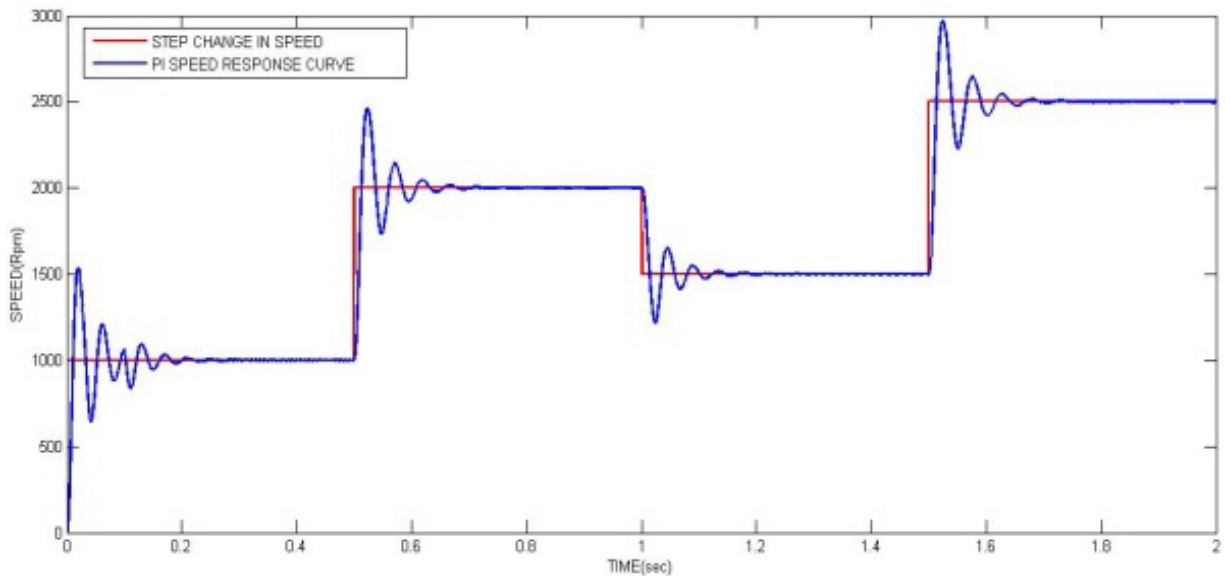
Table 5: Sudden change in speed response curve

Controller techniques	Peak over shoot (rpm)	Peak under shoot (rpm)	Settling time in (sec)	Rise time status
Conventional PI	610	492	0.715	Good
Fuzzy	45	0	0.512	Very good

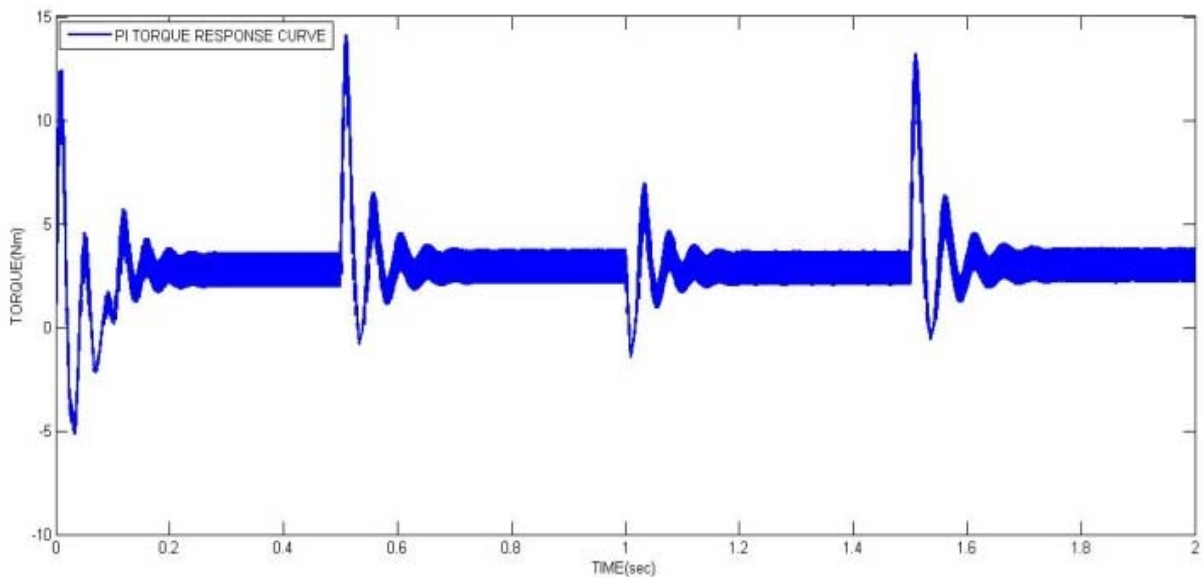
Table 3 shows the mode of operation of the circuit components. Mode 1 to 3 is depicted in Table 3. Table 3 clearly shows the status and working functionality of the switches S1, S2, S3 and S4. In Mode 1, T2a decreases linearly where as T2c increases linearly. It is observed that, IIN increases linearly. In Mode 2, switch S4 is in OFF condition at the end of the time and IIN increases linearly. In Mode 3, S2 is in ON condition and S3 is also in ZVS mode ON condition. IIN and T2a are observed to decrease linearly. T2c and T1a is observed to increase linearly where as T1b decreases linearly. Similar to Table 3 and 4 shows the

modes of operation of the circuit components from Mode 4 to 6. In mode 4, S2 and S4 are ON. Moreover, IIN, T1a, T1b and T2a are observed to increase linearly. T2c decreases linearly (Table 5).

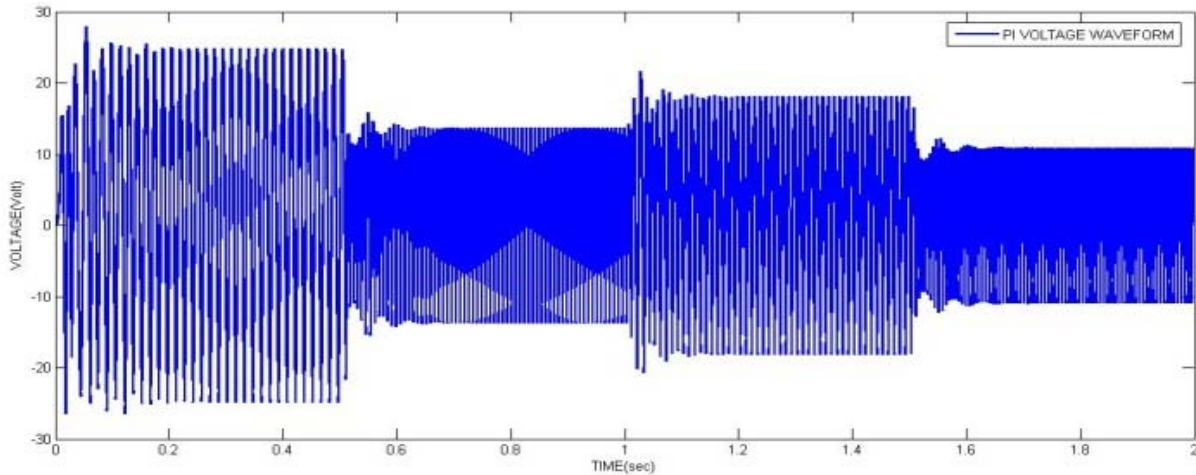
In Mode 5, S2 is observed OFF (End of the time) where as IIN increases linearly. T2a and T2c are in NULL status. Table 2 also shows the Mode 6 operation conditions of the circuit components. It is clearly observed that, S1 is in ZVS mode ON condition whereas S2 is OFF at the beginning time. S3 is in OFF condition and S4 is in ON condition. IIN and T2c decreases linearly where as T2a increases linearly.



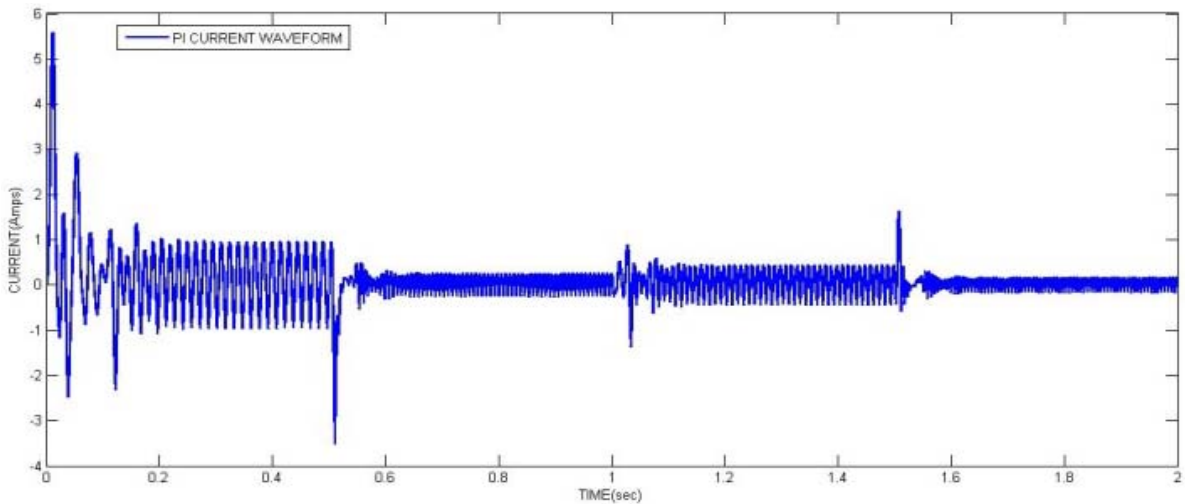
(a) Speed response



(b) Torque response



(c) Voltage response



(d) Current response

Fig. 10: Speed, torque, voltage and current response of PI controller

Table 6: Sudden change in torque response curve at 5 Nm

Controller techniques	Torque at 5 Nm			Speed response
	Peak over shoot (rpm)	Peak under shoot (rpm)	Settling time in (sec)	
Conventional PI	73	148	1.65	Good
Fuzzy	45	60	1.54	Very good

SIMULATION RESULTS AND DISCUSSION

The proposed approach has been simulated in MATLAB R 2011a. Figure 8 shows the simulation diagram of the proposed approach. The performance of the proposed approach has been evaluated based on current, voltage, speed and torque. The evaluations have been carried out for three different Rpm such as 1000, 1500 and 2000, respectively. The simulations have been carried out and waveforms for current, voltage, speed and torque have been attained for two different controllers such as PI and fuzzy.

PI response: Figure 10 shows the overall responses of speed, torque, voltage and current. The waveforms are obtained for the individual response. Figure 10a and b show the speed and torque responses respectively. During speed change, the peak overshoot, peak under shoot, rise time, settling time, etc., gets affected which in turns affects the overall performances of the load (Table 6). When considering the voltage and current response, it is clearly observed that It is observed that, when speed is lesser, current is higher and voltage is lesser. But, when speed is higher, current is lesser and voltage is higher.

Table 7: Sudden change in torque response curve at 4 Nm

Controller techniques	Torque at 4 Nm			
	Peak over shoot (rpm)	Peak under shoot (rpm)	Settling time in (sec)	Speed response
Conventional PI	80	60	2.126	Good
Fuzzy	40	0	2.042	Very good

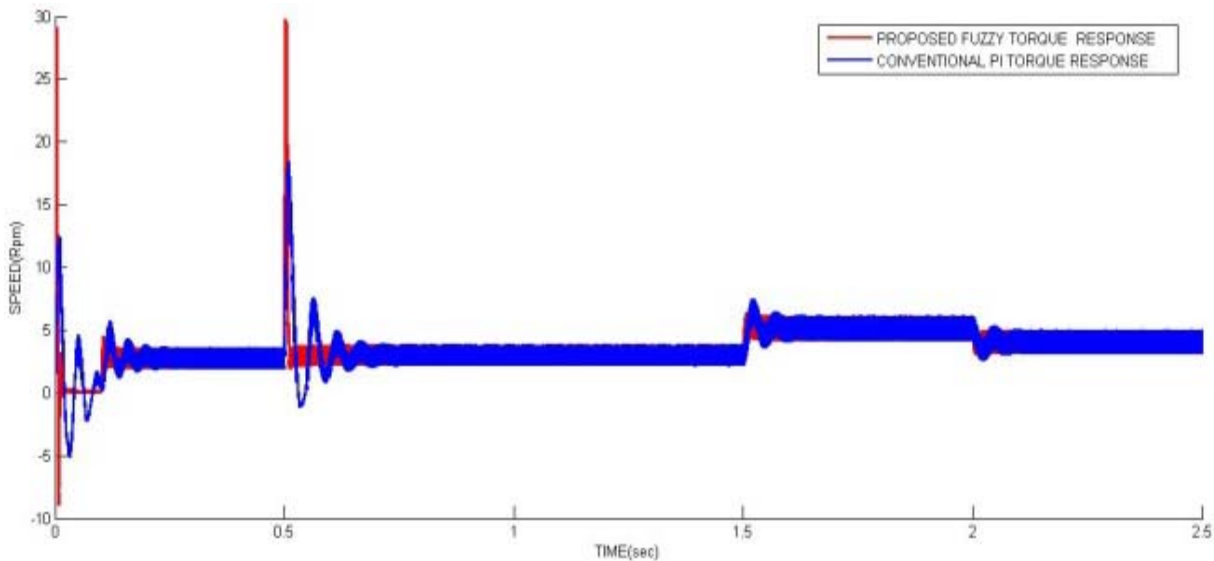


Fig. 11: DC link voltage response comparison

Fuzzy response: Figure 5 shows the overall responses of speed, torque, voltage and current for the fuzzy controller. Figure 5a and b show the speed and torque responses respectively for the fuzzy controller. The waveforms for the step change in speed and its response is clearly shown in the Fig. 5.

Speed response comparison: Figure 6 clearly shows the combined speed response of the PI and Fuzzy controllers for different step change. It is observed from the figure that the proposed fuzzy based speed response curve provides better results when compared with the PI based response. The ripples of the proposed fuzzy based response are observed to be lesser when compared with the PI response. For all the three rpm such as 1000, 1500, 2000 and 2500, respectively the peaks overshoot, peak undershoot, settling time, rise time is observed to be significant with the fuzzy controller.

Sudden change in speed with sudden change in torque: Figure 7 clearly shows the combined speed response of the PI and Fuzzy controllers. The waveforms are obtained for different speed and torque response. The speed responses are evaluated at 0.5 seconds. The torque variations are formed at 1.5 and 2 sec. The individual responses of the fuzzy and PI controllers for the speed and torque variations have been shown in Fig. 7. Figure 4 shows the clearly shows the depiction of the fuzzy and PI controller responses. The Torque variation is carried out at 3, 4 and 5 NM,

respectively and the responses for each NM is been evaluated. The peak overshoot and settling time response has been evaluated and depicted in the Fig. 4 and Table 7.

Table 5 shows the overall speed response curve of the PI and fuzzy controller. The performance is evaluated for Peak overshoot, Peak under shoot, settling time and rise time. It is observed from the table that the peak overshoot of the conventional PI and fuzzy controller is observed to be 610 and 45 rpm, respectively. The settling time of the PI and fuzzy controller is observed to be 0.715 and 0.512 sec, respectively. Moreover, the peak under shoot of the conventional PI and fuzzy is observed to be 492 rpm and zero respectively.

Combined torque response: Figure 11 shows the combined torque response of the conventional PI and proposed fuzzy based controller approach. Torque response of the proposed fuzzy controller is observed to outperform the conventional PI controller.

Figure 12 shows the speed torque relation of the proposed approach. It is evident that when there is sudden change in speed, the torque remained constant. But, with sudden change in torque, the speed is kept constant. Figure 11 shows the comparison and the relational analysis of Step Change vs. Speed response of the PI controller and fuzzy controller respectively. It is clearly observed from the graph that the fuzzy controller provides significant results when compared with the PI controller. The performance of the fuzzy

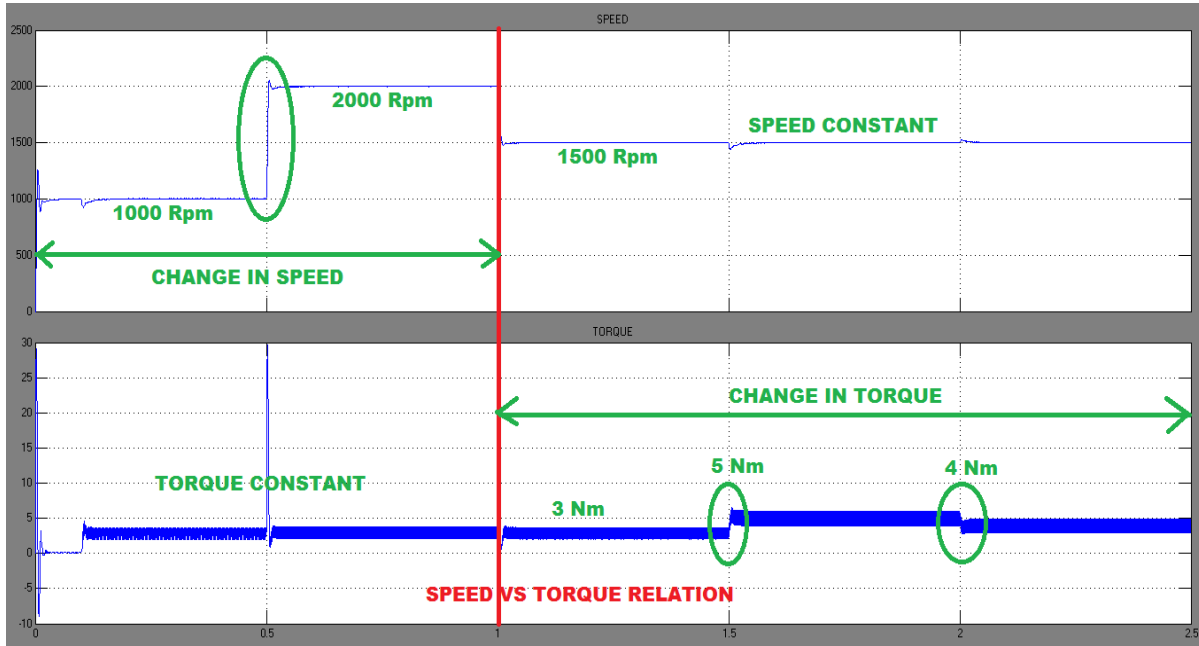


Fig. 12: Speed torque relation

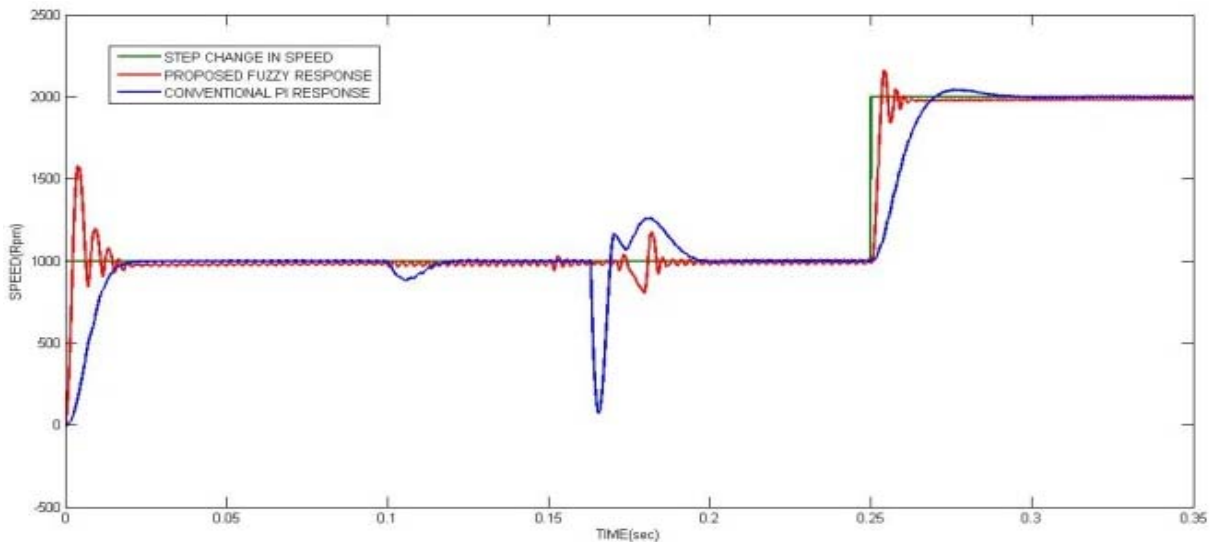


Fig. 13: Fault response

controller is significant in terms of the rise time, settling time and peak overshoot.

Figure 13 shows the fault analysis with single leg failure and two leg failure in the inverter. It is clearly observed that single leg failure is created at 0.12 sec, the recovery of the PI controller takes some time, but the fuzzy controller provides significant results with lesser settling time.

Similarly, two leg failures are created at 0.17 sec; the fault recovered by the PI controller takes higher time for settling with higher peak overshoot. But, the fuzzy controller takes lesser settling time with lower peak overshoot.

Table 8 shows the fault recovery analysis of the PI and fuzzy controller techniques for single switching failure (Fig. 14). The failure occurred at 0.1 sec and it is observed that, peak under shoot obtained for conventional PI controller is 210 rpm, whereas for fuzzy it is 10 rpm. Moreover, the settling time taken by the conventional PI is 0.12 sec whereas for fuzzy it is 0.105 sec.

Table 9 shows the switching failure with two leg two switching failure. It is observed that peak overshoot attained for PI controller is 261 rpm whereas for fuzzy approach, it is 143 rpm. Peak under shoot attained by the PI controller is 982 rpm whereas for fuzzy

Table 8: Fault recovery analysis with single switch failure

Controller techniques	Single switch 0.1 sec			
	Peak over shoot (rpm)	Peak under shoot (rpm)	Settling time in (sec)	Speed response
Conventional PI	0	210	0.120	Good
Fuzzy	0	10	0.105	Very good

Table 9: Fault recovery analysis with single switch failure

Controller techniques	2 leg 2 switching failure 0.16 sec			
	Peak over shoot (rpm)	Peak under shoot (rpm)	Settling time (sec)	Speed response
Conventional PI	261	982	0.210	Good
Fuzzy	143	248	0.175	Very good

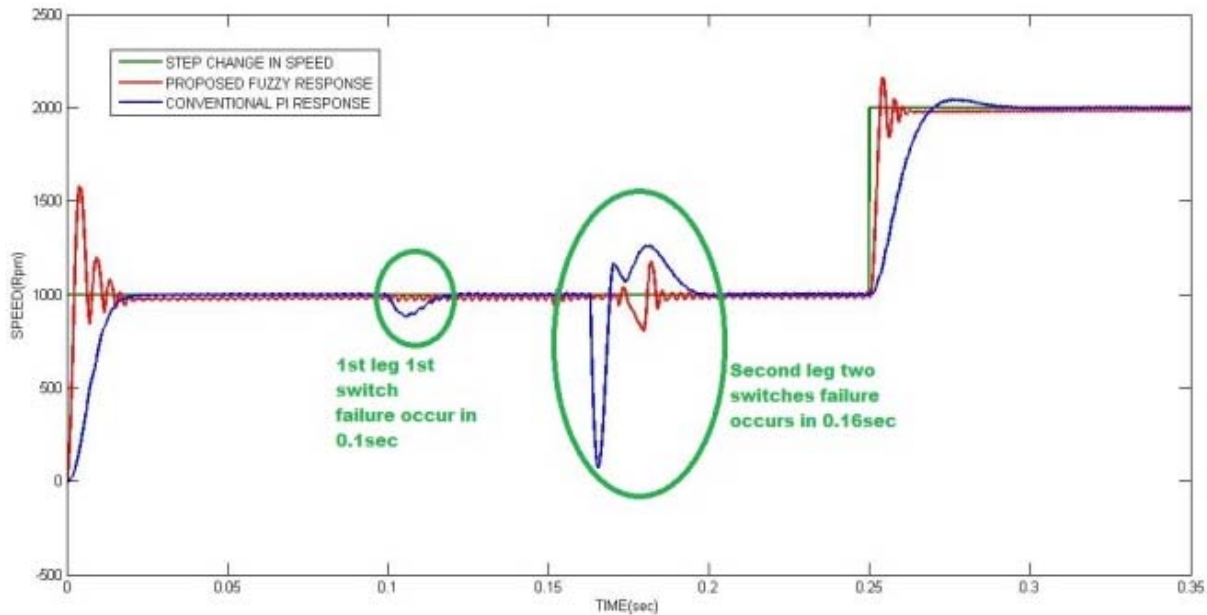


Fig. 14: Fault analysis

controller it is 248 rpm. Similarly, the settling time is also lesser for the proposed fuzzy approach. The speed response of the proposed fuzzy controller is significant when compared with the conventional PI controller.

CONCLUSION

Fault analysis and recovery in BLDC motor has become an active area of research in the field of power electronics. A number of works have been carried out in this application, but still there is always a scope for improvement. This research work focuses on the fault analysis and recovery of the BLDC motor when the leg failure occurs in the inverter. For this approach, two controllers have been utilized. Moreover, in order to reduce the power consumption in the load side, HGHC has been used for which the input is taken from the back emf. The simulation results show that the proposed approach provides significant results in terms of speed variation, settling time, peak overshoot and rise time. The torque speed relational variation is observed to be very significant in this proposed approach.

REFERENCES

- Alaeinovin, P. and J. Jatskevich, 2012. Filtering of hall-sensor signals for improved operation of brushless DC motors. *IEEE T. Energy Convers.*, 27(2): 547-549.
- Alcazar, Y.J.A., D. de Souza Oliveira, F.L. Tofoli and R.P. Torrico-Bascope, 2013. DC-DC nonisolated boost converter based on the three-state switching cell and voltage multiplier cells. *IEEE T. Ind. Electron.*, 60(10): 4438-4449.
- Awadallah, M.A. and M.M. Morcos, 2004. ANFIS-based diagnosis and location of stator inter-turn faults in PM brushless DC motors. *IEEE T. Energy Convers.*, 19(4): 79-796.
- Bouzelata, Y., H. Djeghloud and R. Chenni, 2012. The application of an active power filter on a photovoltaic power generation system. *Int. J. Renew. Energ.*, 2(2): 583-590.
- Gamazo-Real, J.C., E. Vázquez-Sánchez and J. Gómez-Gil, 2010. Position and speed control of brushless DC motors using sensorless techniques and application trends. *Sensors (Basel)*, 10(7): 6901-6947.

- Hubik, V., M. Sveda and V. Singule, 2008. On the development of BLDC motor control run-up algorithms for aerospace application. Proceeding of the 13th Power Electronics and Motion Control Conference (EPE-PEMC, 2008). Poznan, Poland, pp: 1620-1624.
- Iizuka, K., H. Uzuhashi, M. Kano, T. Endo and K. Mohri, 1985. Microcomputer control for sensorless brushless motor. IEEE T. Ind. Appl., 1A-21(4): 595-601.
- Je-Wook, P., A. Woo-Young, K. Jang-Mok and H. Byung-Moon, 2013. Sensorless control algorithm of BLDC motors with current model. Proceeding of the IEEE International Conference on Industrial Technology (ICIT), pp: 1648-1652.
- Kinjo, T., T. Senjyu, N. Urasaki and H. Fujita, 2006. Output leveling of renewable energy by electric double-layer capacitor applied for energy storage system. IEEE T. Energy Convers., 21(1): 221-227.
- Luiz, S.H., C. Barreto, P.P. Paulo, Demercil, S. Oliveira and S.N.A.L. Ranoyca, 2014. High-voltage gain boost converter based on three-state commutation cell for battery charging using PV panels in a single conversion stage. IEEE T. Power Electr., 29(1).
- Tingna, S., G. Yuntao, S. Peng and X. Changliang, 2010. A new approach of minimizing commutation torque ripple for brushless DC motor based on DC-DC converter. IEEE T. Ind. Electron., 57(10): 3483-3490.
- Torrice-Bascope, G.V., S.A. Vasconcelos, R.P. Torrice-Bascope, F.L.M. Antunes, D.S. de Oliveira and C.G.C. Branco, 2006. A high step-up DC-DC converter based on three-state switching cell. Proceeding of the IEEE International Symposium on Industrial Electronics, 2: 998-1003.
- Yaonan, W., Z. Xizheng, Y. Xiaofang and L. Guorong, 2011. Position-sensorless hybrid sliding-mode control of electric vehicles with brushless DC motor. IEEE T. Veh. Technol., 60(3): 421-432.
- Zhenyu, H., 2012. A control method of AC induction motor based on CMAC and single neuron PID controller. Proceeding of the International Conference on Control Engineering and Communication Technology (ICCECT, 2012), pp: 253-258.